VOL. 13, NO. 4 J. HYDRONAUTICS OCTOBER 1979
ARTICLE NO. 78-757R

Application of Hybrid Composites to Hydrofoil Structures

L. B. Greszcuk*
McDonnell Douglas Astronautics Company, Huntington Beach, Calif.
A. V. Hawley†
Douglas Aircraft Company, Long Beach, Calif.
and
W. Couch‡
Naval Ship Research and Development Center, Carderock, Md.

Studies are presented on application of advanced composites to hydrofoil structural components such as struts and foils. It is shown that to satisfy the strut/foil structural requirements and constraints, the most cost-effective and structurally efficient designs are achieved by using hybrid composites consisting of a combination of high-strength and high-modulus graphite fibers. Typical curves are presented for determining the various mechanical properties of hybrid composites as a function of the amounts and orientations of the constituent materials. To make a realistic assessment of efficiency of hybrid composites as applied to hydrofoil structural components, the various mechanical properties of 0.5-in. thick multilayer, multidirectional hybrid composites are evaluated experimentally. The experimental results for strength and elastic properties of hybrid composites show excellent correlation with predictions and verify the efficiency of these materials as applied to structural components of advanced naval hydrostructures. Preliminary results are also presented on fabrication and testing of a 60-in. long, hybrid composite, tapered box beam structure simulating the forward foil on the PCH.

Introduction

ADVANCED composites such as boron-epoxy and graphite-epoxy have been successfully employed as structural materials for aircraft, missiles, and space vehicles and have performed satisfactorily as demonstrated through extensive ground testing and in-flight performance. Use of composites in the above noted applications has resulted in weight savings of 11-50%. Because of these weight savings, resultant improvements in systems performance, and continuing decreases in cost of fibers and prepregs, the advanced composites have reached the stage of development where they are now being used on production military aircraft and undergoing flight tests on commercial aircraft.

Results obtained during recent studies[1,2] show that for structural components of advanced naval hydrostructures such as hydrofoils, weight savings similar to those achieved in aircraft are possible through application of advanced composites to hydrofoil structural components such as struts, foils, decking, and hull structure. Used individually, the various composites offer weight savings at a relatively high cost per pound of finished structure; only through hybridization of different composites does it appear feasible to achieve significant weight savings at a minimum cost, as discussed in the sections that follow.

Presented as Paper 78-757 at the AIAA/SNAME Advanced Marine Vehicles Conference, San Diego, Calif., April 17-19, 1978; submitted July 28, 1978; revision received June 4, 1979.

Index categories: Marine Materials Corrosion/Erosion; Marine Vessel Design (including Loads); Marine Vessel Systems, Submerged and Surface.

*Principal Engineer/Scientist, Advanced Structures and Mechanical Dept. Member AIAA.
†Senior Engineer/Scientist, Structures Engineering.
‡Structural Engineer, Structures Dept., Surface Ship Division.

General Description

The overall view of the hydrofoil under consideration is shown in Fig. 1. The full load displacement of the hydrofoil is approximately 280,000 lb, of which 40% is for the hull structure and foil system; 20% is for payload; 15% is for propulsion; and the remaining 25% is for electrical plant, communications and control, nonstructural auxiliary systems, outfits and furnishings, fixed armaments, and miscellaneous items. Materials used for the various components of the PCH are aluminum for the hull structure and HY80/HY130 steel for the foils and struts. Because of the availability of information for the existing PCH, such as design loads, safety factors, weight breakdown, operational characteristics, and other requirements, the various tradeoff studies that were conducted were based on—and the results of these studies compared to—the existing PCH design. The results can, however, be used to make preliminary estimates of the payoffs resulting from using composites in more advanced hydrofoils.

Application of Composites to Forward Foil and Strut

Two of the hydrofoil structural components for which applicability of advanced composites was investigated in some detail were the forward strut and the foil. The composite designs were constrained to have the same external geometries as the existing parts and to be fully interchangeable with them. No changes were made to the control surfaces or their operating mechanism the investigation being confined to the fixed structural portions only. The geometry of the strut is shown in Fig. 2, while Fig. 3 shows the geometry of the foil. The lower portion of the strut has a 12% thickness-to-chord ratio, increasing to 20% at the upper end. The foil surface area and aspect ratio are 65.6 ft^2 and 6.1, respectively. The sweepback measured on the 25% chordline is 15 deg, and the flap hinge line is on the 75% chordline. The foil has a 9% thick NCA 16-309 section with a maximum thickness of 5.67 in. at the root end. The weight of the steel strut and foil are 2173 lb and 2714 lb, respectively. The critical loads acting on

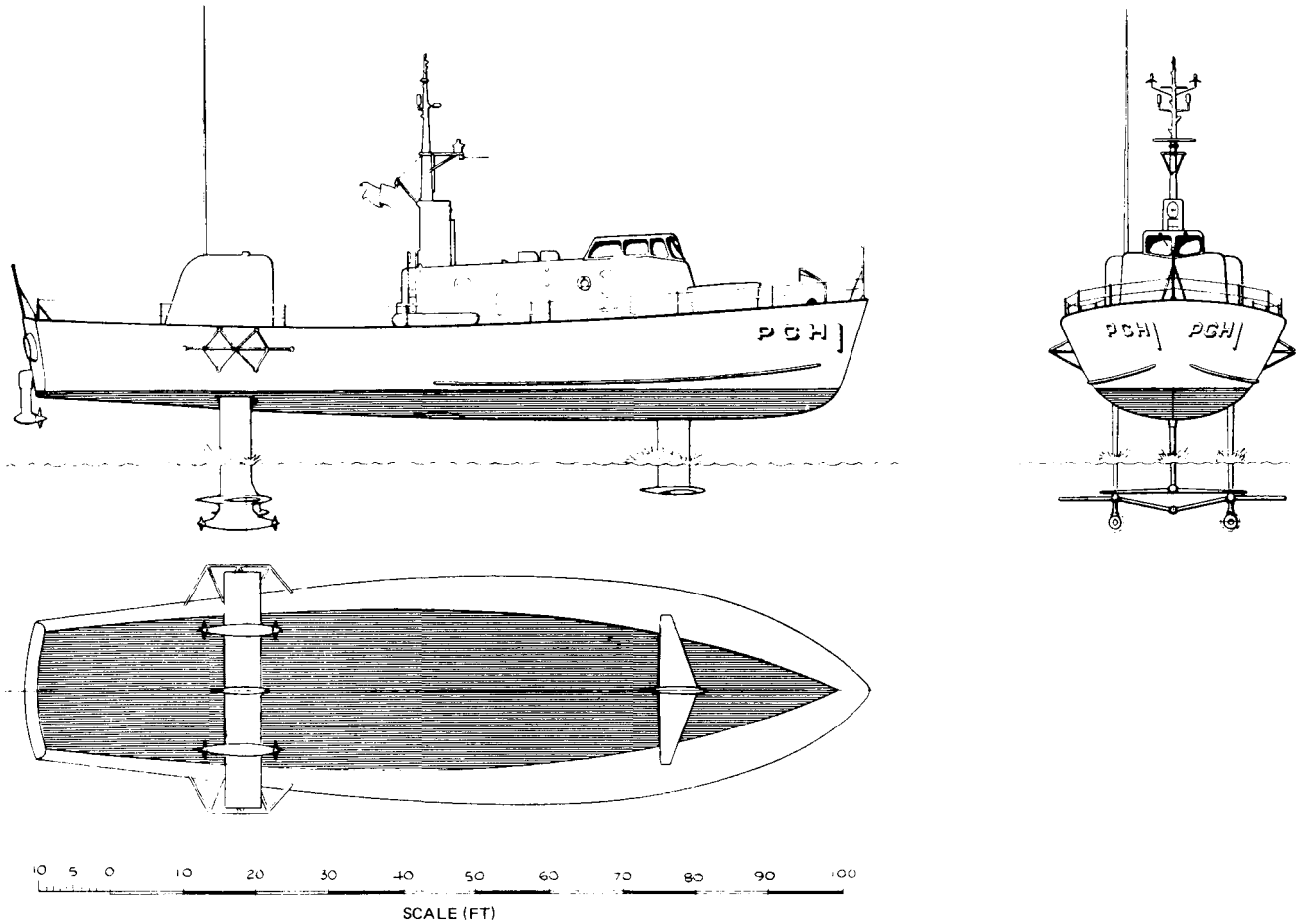

Fig. 1 Overall view of the patrol craft hydrofoil (PCH).

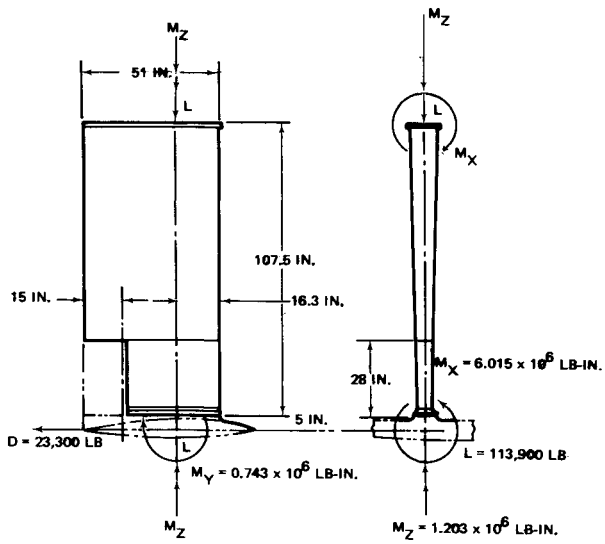

Fig. 2 Strut geometry and critical loads.

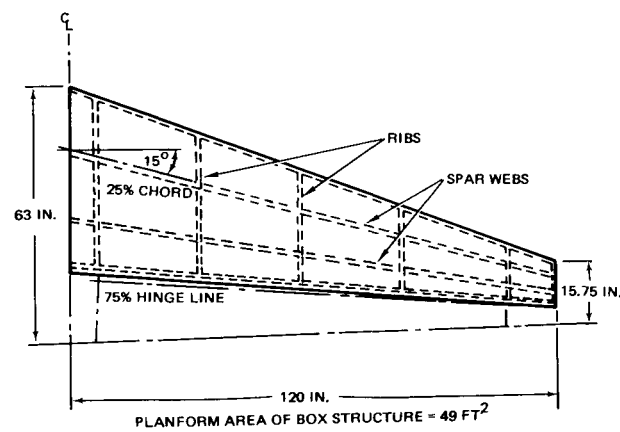

Fig. 3 Forward foil geometry.

the strut and the foil are shown in Fig. 2. They correspond to the worst condition and were derived from Ref. 3. In contrast to a specified safety factor of 1.25 for metal components,[3] a safety factor of 1.5 was used when designing the composite components.

In designing the composite foil and strut it was found that in addition to meeting the strength requirements dictated by the design limit and critical load conditions, the structures also had to meet certain bending and torsional requirements dictated by consideration of flutter, divergence, and flap reversal speeds. In connection with the latter, the operating speed of PCH was assumed to be 50 knots. Thus, the requirements for the design of the foil and the strut were: 1) tensile and compressive strengths, 2) hydroelastic flutter, 3) divergence, and 4) flap reversal speed. Items 2, 3, and 4 were expressed in terms of the geometries and the required EI and GK at the critical section of each component. Knowing the required EI and GK and the critical bending moment, it was possible to plot the required values of Young's modulus E, shear modulus G, and the maximum tensile (F_t) and compressive stresses (F_c) at the extreme fiber (c = 3.06 in.) as a function of the wall thickness, as shown, for example, in Fig. 4. As the twisting moment and thereby shear stresses were

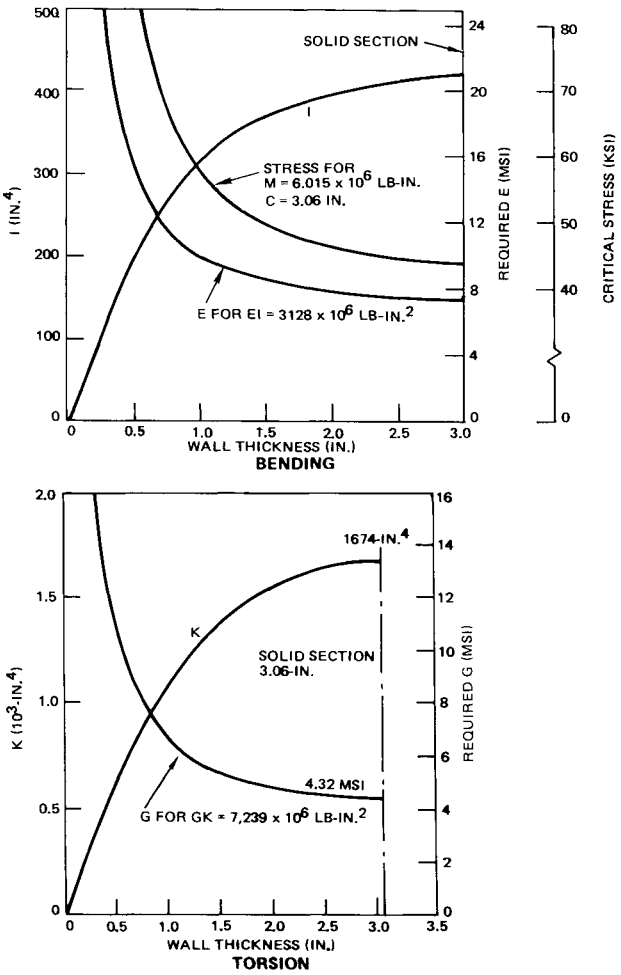

Fig. 4 Bending and torsional properties for the strut.

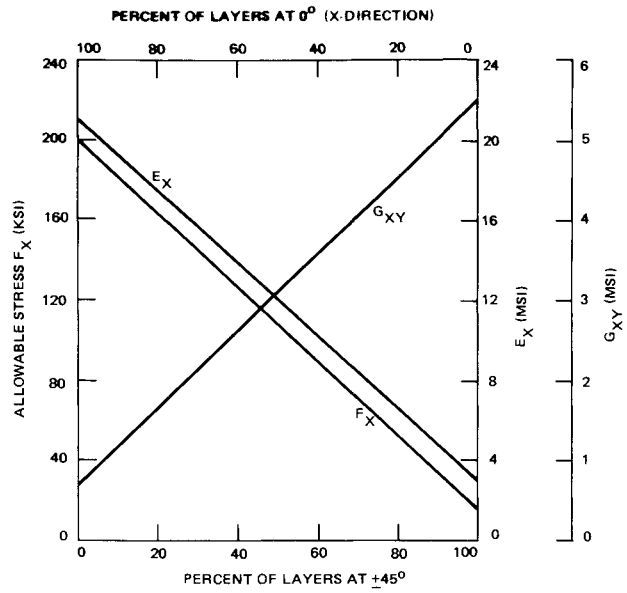

Fig. 5 Properties of multidirectional composites made with Thornel 300 epoxy.

quite small (see Fig. 2), it was found that the thickness to satisfy shear requirements was dictated totally by shear stiffness rather than by shear stresses. To establish which composites and combinations of composites and layups would give the required properties, curves of the form shown in Fig. 5 were prepared for composites and different combinations of composites shown in Table 1. In the initial comparative studies, it was assumed that all layers would be aligned in either 0 deg lengthwise direction or at ±45 deg. This layup was found to satisfy the strength requirements as well as the bending and torsional stiffness requirements.

By combining the material property charts, such as shown in Fig. 5, with E, G, and stress charts, such as shown in Fig. 4, plots were obtained for the acceptable region of wall thickness against the percentage of layers at ±45 deg for each material combination. Figure 6 shows the final results for the required wall thickness of a strut made of Celion GY70/epoxy, while Fig. 7 shows similar results for a strut made of Thornel 300/epoxy. In the case of all GY70/epoxy struts (Fig. 6), the minimum wall thickness to satisfy the various design requirements is $t = 1.51$ in. and is governed by the torsional rigidity and strength requirements. To satisfy the bending stiffness and torsional rigidity, a thickness of only $t = 0.74$ in. would be required. Thus, the design is penalized because of the inadequate strength of GY70/epoxy.

In the case of struts made from Thornel 300/epoxy, the minimum wall thickness to satisfy the various requirements is $t = 3.02$ in. for the case of dispersed construction and is governed by the torsional rigidity and bending stiffness. As noted in Fig. 7, the wall thickness can be reduced to $t \approx 2.5$ in. if part of the unidirectional material is placed near the outer surface of the strut. Again, if it were not for the low bending stiffness, a thickness of less than 2 in. would be satisfactory. Here the design is penalized by the inadequate stiffness of the Thornel 300/epoxy. The results presented in Figs. 6 and 7 identified the strengths and weaknesses of the two materials

Table 1 Material properties used in design

Material	Modulus, Msi				Strength, ksi				
	E_L	E_T	G_{LT}	ν_{LT}	σ_{tL}	σ_{cL}	σ_{tT}	σ_{cT}	σ_{LT}
Steel	29	29	11	0.33	*	*	*	*	*
S-Glass	8	2.2	0.9	0.26	280	170	11	20	9
PRD 49-III	11	0.9	0.3	0.30	180	40	5	20	8
Boron (AVCO 5505)	30	2.8	1.0	0.21	180	250	9	30	13
Graphite									
Thornel 75	42	0.9	0.7	0.32	170	90	4	20	9
Celion GY70	42	0.9	0.7	0.32	90	90	3	27	9
Narmco 5206 Type II	21	1.3	0.7	0.21	160	160	7	29	10
Thornel 300/ Narmco 5208	21	1.3	0.7	0.25	210	200	8	33	13

*The critical steel stress is the yield stress given by the HY number (e.g., 100 for HY 100).

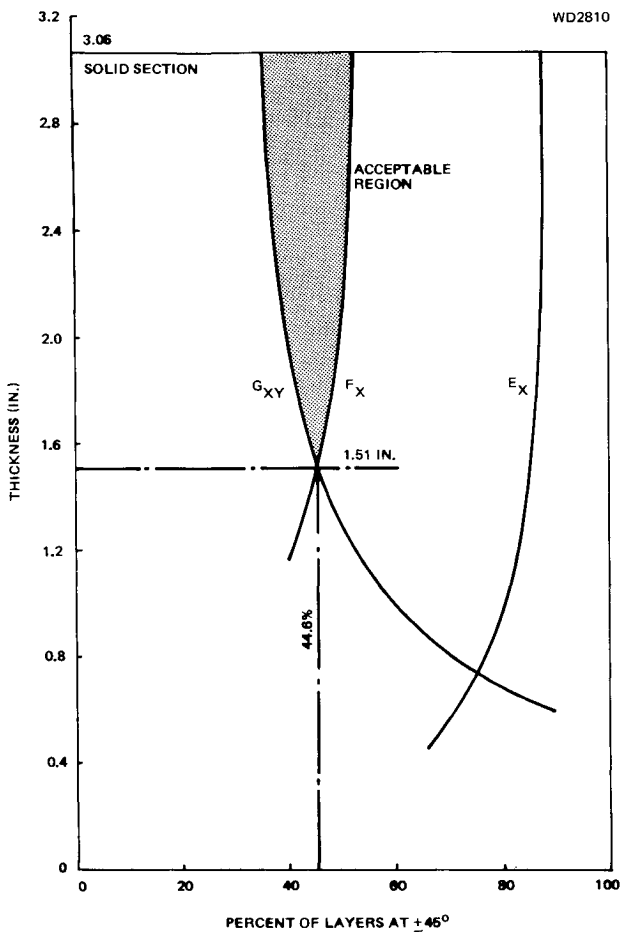

Fig. 6 Required thickness of strut shell made of Celion GY70/epoxy.

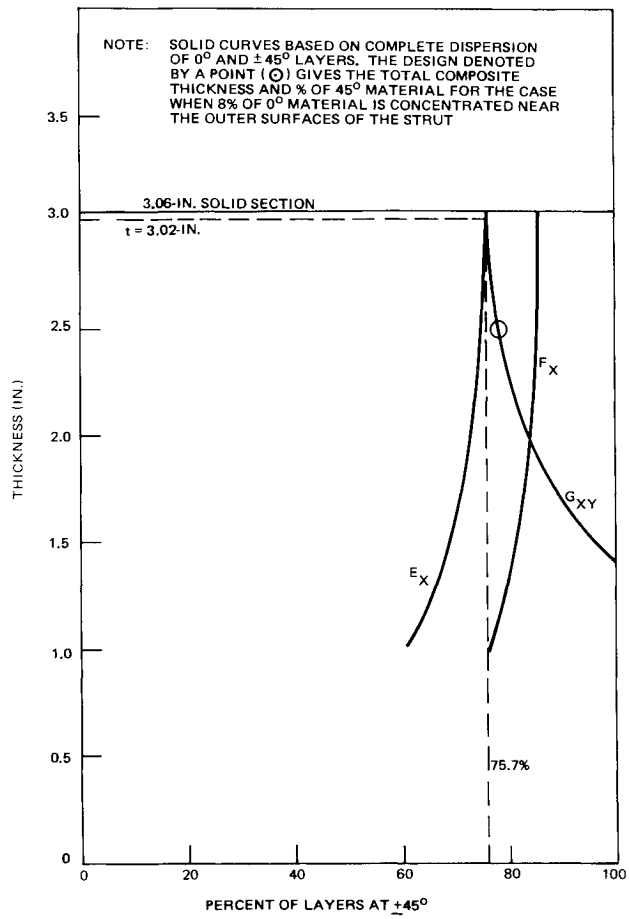

Fig. 7 Required thickness of strut shell made of Thornel 300/epoxy.

when used individually and led to the idea of combining the materials into a hybrid composite in which one of the constituents would satisfy stiffness requirements and the other satisfy strength requirements. The results for the required wall thickness of the strut made of a GY70/Thornel 300 hybrid composite are shown in Fig. 8. Comparing the results shown in Figs. 6, 7, and 8 shows that hybridization minimizes the shell wall thickness and thereby the structural weight.

To establish the influence of hybridization on cost, partial cost estimates were made for the strut shell designs employing different materials. No attempt was made at this stage to estimate the total costs, but the various configurations were compared by considering only those costs that depended on the design changes. It was assumed that all the significant variable costs were associated with the amount of composite material used, and that other costs such as tooling, machining, and autoclave operation and preparation remained constant. Based on past experience, the total layup and inspection costs were taken at \$60/lb of finished composite. Assuming material waste of 60%, the total variable cost C_v for struts made of different composites became

$$C_v = \$(60 + 1.6C)\ W$$

where W is the weight of the finished laminate and C is the cost per lb of prepreg.

To make a comparison with the existing steel components, an equivalent cost was required for the fabrication of these parts. The latter was estimated as \$10/lb in 1974, rising to \$13.50/lb in 1980 due to increasing material and labor prices.

Table 2 Weight and cost[a] comparison of strut shell materials

Material	Thickness, in.	Layer direction, deg	Percentage of layers	Volume, cu in.	Weight, lb	Weight saving, %	Cost, \$ 1974	Cost, \$ 1980
Steel	0.50			5,000	1,420	. . .	14,200	19,100
Boron	1.18	0/±45	24.3/75.7	11,600	836	41.1	237,500	117,000
Thornel 75	1.23	0/±45	48.5/51.5	12,100	678	52.2	268,600	95,000
Celion GY-70	1.51	0/±45	54.4/45.6	14,600	818	42.4	114,400	81,800
Boron	0.86	0	34.0	2,920	210	62.8	59,600	29,400
Celion GY-70		±45	66.0	5,680	318		44,500	31,800
				8,600	528		104,100	61,200
Thornel 300	0.99	0	40.5	3,970	222	61.4	34,600	19,300
Celion GY-70		±45	59.5	5,830	327		45,800	32,700
				9,800	549		80,400	52,000

[a] Partial cost.

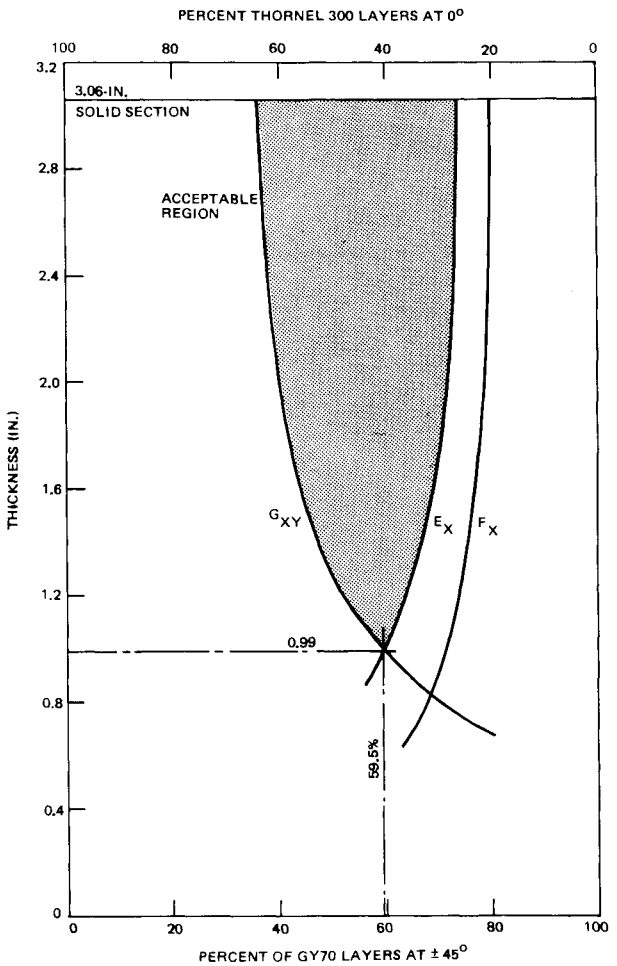

Fig. 8 Required wall thickness of GY70/Thornel 300 hybrid composite strut.

The results, showing a comparison of the partial cost struts made from different materials, are presented in Table 2. In addition to the previously mentioned materials (GY70 and Thornel 300), Table 2 also contains pertinent results for struts made of boron/epoxy, Thornel 75/epoxy, and boron/epoxy-GY70/epoxy hybrid composites. Results similar to those shown in Table 2 were also obtained for the forward foil. Tables 3 and 4 show the influence that hybridization has on the relative weight and cost of the hydrofoil strut shell and the foil shell. As can readily be seen, hybridization offers a design at minimum weight and minimum cost.

Results such as those shown in Table 2 were used for selecting optimum materials and combinations of materials for efficient, cost-effective strut and foil designs. Following the selection of materials, more detailed design and analysis studies were conducted on the foil and the strut. This included further optimization of layout and distribution of the selected materials, design of internal structure for the foil and the strut, design and analysis of all primary and secondary joints and attachments, access openings, etc. Preliminary design drawings were then prepared for each of the components. These were used for obtaining more accurate weight and cost estimates than those obtained in the more generalized analyses. The final cost figures for the components included cost of composite materials, steel, scrap (waste), and all cost associated with fabrication and assembly, quality control, tooling, and planning. Included also in the cost estimate were allocations, overlays, and allowances which were predicted by the conventional manufacturing methods. References 1, 2, and 4 contain more detailed descriptions of the final design and of results.

Table 3 Influence of hybridization on the relative weight and cost of a hydrofoil strut shell

Material	Shell wall thickness, in.	Relative weight	Relative cost
Steel	0.50	1.0	1.0
Celion GY70/epoxy	1.51	0.576	8.0
Thornel 300/epoxy	≈2.50	>0.88	13.8
Hybrid composite (Celion GY/70 Thornel 300/epoxy)	0.99	0.386	5.6

Table 4 Influence of hybridization on the relative weight and cost of the forward foil

Material	Shell wall thickness, in.	Relative weight	Relative cost
Steel	0.57	1.0	1.0
Celion GY70/epoxy	2.07	0.61	8.6
Thornel 300/epoxy (solid section)	2.84	0.75	11.7
Hybrid composite (Celion GY/70 Thornel 300/epoxy)	1.28	0.42	6.1

Experimental Studies on Hybrid Composites

To demonstrate that the predicted benefits inherent to hybrid composites could be achieved, 0.5-in. thick hybrid composite panels were fabricated, and test coupons excised from the panels were tested to obtain the various strength and elastic properties. The panels consisted of 53 plies (≈58%) of Thornel 300/5208 at 0 deg orientation and 32 plies (≈42%) of GY70/5208 at ±45 deg orientation. The 85 plies making up the 0.5-in. thick hybrid composite were dispersed according to the following layup:

$$\left[0^\circ, (0_3^\circ, \pm 45^\circ)_8, 0_3^\circ, (\pm 45^\circ, 0_3^\circ)_8, 0^\circ)\right]$$

A typical panel was fabricated by first laying up an oversized panel 0.125 in. thick, staging the latter at 250°F, cutting it into four sections, stacking the sections, instrumenting with thermocouples, and vacuum bagging and curing in the autoclave according to a predetermined cure cycle. Upon completion, appropriate NDE tests were conducted. Fiber, resin, and void content determinations were also made, as were also measurements of in situ thickness per ply and variation of fiber and resin content through the thickness of the panel. Figure 9 shows a typical cross section of a 0.5-in. thick hybrid composite panel. The thickness per ply and ply distribution appears to be fairly uniform through the thickness of the panel. Several of the failed hybrid composite test specimens are shown in Fig. 10. The arrows shown above the specimens denote the direction of the 0 deg Thornel 300 layers. As can be seen in Fig. 10, most of the specimen configurations worked satisfactorily. One exception was the transverse specimens (third from left in Fig. 10), which failed near the doubler. Typical stress-strain curves for specimens subjected to tensile and compressive loading in the direction of Thornel 300 layers (0 deg direction) are shown in Fig. 11. In tension, the material exhibited linear stress-strain behavior up to failure. Some nonlinearity was observed in the stress-strain behavior under compressive loading. The compressive Young's modulus of the hybrid composite was slightly lower than the tensile modulus. Table 5 contains the measured

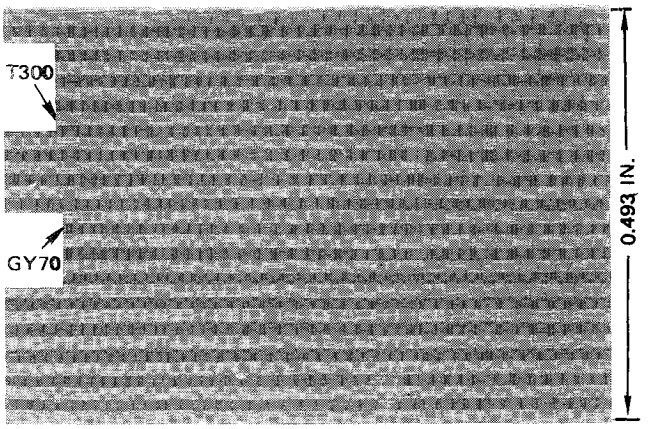

Fig. 9 Typical cross section of a hybrid composite consisting of Thornel 300/5208 at 0 deg and Celion GY70/5208 at ±45 deg.

NOTE: ARROW (▲▼) DENOTES DIRECTION OF 0° THORNEL 300 LAYERS.

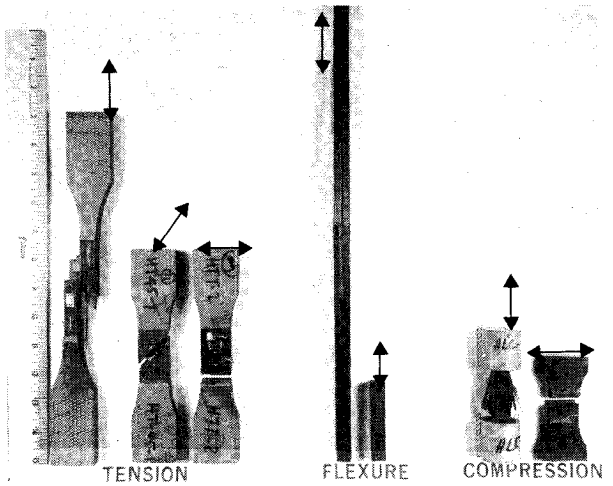

Fig. 10 Failed hybrid composite test specimens.

properties data for hybrid composites as well as the theoretically predicted values. The latter were calculated using average properties of unidirectional Thornel 300 and GY70 composites given in literature and shown in Figure 12. Shown also in Fig. 12 are generalized carpet plots for tensile and compressive strength, Poisson's ratios, and Young's moduli of hybrid composites. The elastic properties were calculated using conventional techniques such as those described in Ref. 5. The strength properties were calculated by first determining the multiaxial stresses in the various layers of a hybrid composite subjected to some externally applied loading. This was done using lamination theory.[5] For any given layer the stresses were then resolved into stresses associated with the principal axes of symmetry of the material. The latter were then used as inputs in a failure criterion to predict the magnitudes and combinations of stresses required to cause failure of the laminate as well as the mode of failure (i.e., transverse, axial, or shear). Both maximum stress criterion and distortion energy theory applicable to generally orthotropic solids[6] were used as failure criteria. The lower value predicted from the two failure criteria was used as the strength. Externally applied stress causing failure of any given layer within the hybrid composite was taken as the strength of hybrid composite.

A number of important conclusions can be drawn from the excellent test-theory correlation of the properties of hybrid composites. The tests confirm the theoretically predicted properties, and the hybrid composites are as efficient as was

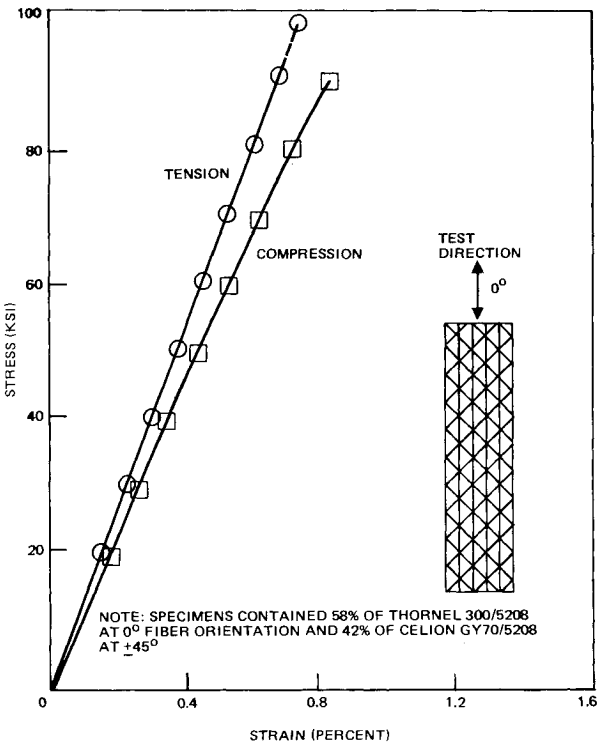

Fig. 11 Typical stress strain curves for Thornel 300/GY70 hybrid composites.

shown in the previous section. No degradation of properties was encountered due to hybridization or because of processing anomalies. The properties of unidirectional composites given in Fig. 12 were obtained from relatively thin laminates ($t \leq 0.125$-in.) and used to predict properties of thick ($t \approx 0.5$-in.) hybrid composite laminates. The fact that predicted properties agree well with test data implies that there was no degradation due to thickness effect.

As to the potential problem of degradation of hybrid composite properties because of water absorption, work to date conducted at NSRDC[7] has shown negligible effect up to one year's soak in sea water. During the one year exposure, no change occurred in the Young's modulus of the hybrid. The interlaminar shear strength decreased ≈3% whereas the flexure strength decreased ≈7%. The decrease in flexure and shear strengths took place during the first four weeks of exposure, following which there was no additional reduction in strength. Work on the effect of exposing hybrid composites and composite/metal joints to sea water is continuing.

Fabrication of Advanced Composite Hydrofoil Test Component (Tapered Box Beam)

To further verify the benefits resulting from application of hybrid composites to hydrofoil structures, a tapered box beam simulating the forward foil was designed and fabricated for experimental evaluation at NSRDC. This test component is typical of the construction and layups that would occur at the midlength of the full-size foil (Fig. 3) if the latter were made of composities. Studies subsequent to those yielding the results shown in Tables 2 and 4 have indicated that the cost of the foil vis-a-vis that of the box beam could be further reduced by making the internal structure out of metal and making only the skins out of hybrid composites. Thus, the final design of the tapered box beam simulating the forward foil consisted of 0.5-in. thick hybrid composite skins (similar to those discussed in the previous section) and HY130 metal substructure. The substructure consisted of a central tapered I-beam and two tapered side channels, all three components being welded at one end to a loading plate where a con-

	THORNEL 300	GY70
PROPERTIES		
E_L (10^6PSI)	20.25	42.0
E_T (10^6PSI)	1.64	0.86
G_{LT} (10^6PSI)	0.85	0.60
μ_{LT}	0.25	0.25
μ_{TL}	0.0202	0.005
STRENGTH		
σ_L(+) KSI	215.0	90.0
(−) KSI	198.0	90.0
σ_T (+) KSI	6.1	3.0
(−) KSI	33.0	27.5
τ_{LT}KSI	12.0	8.6

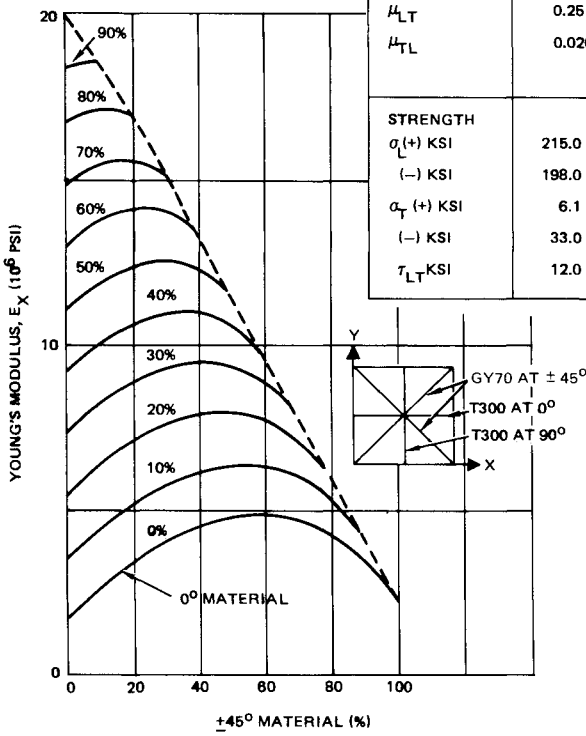

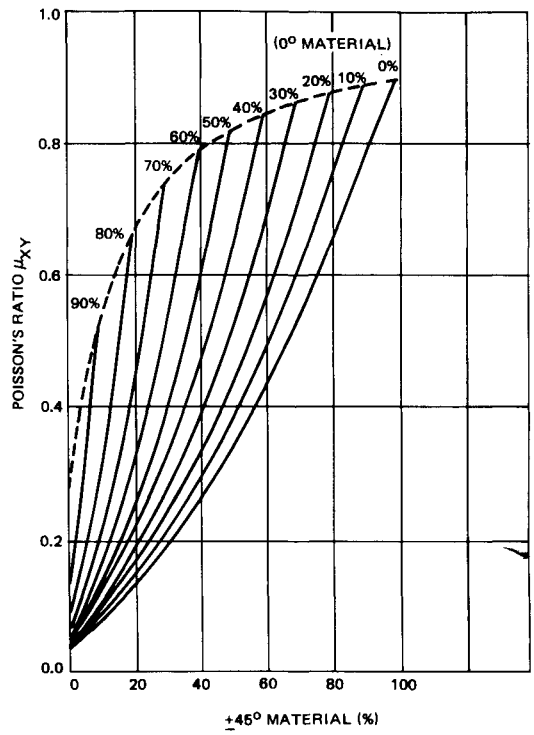

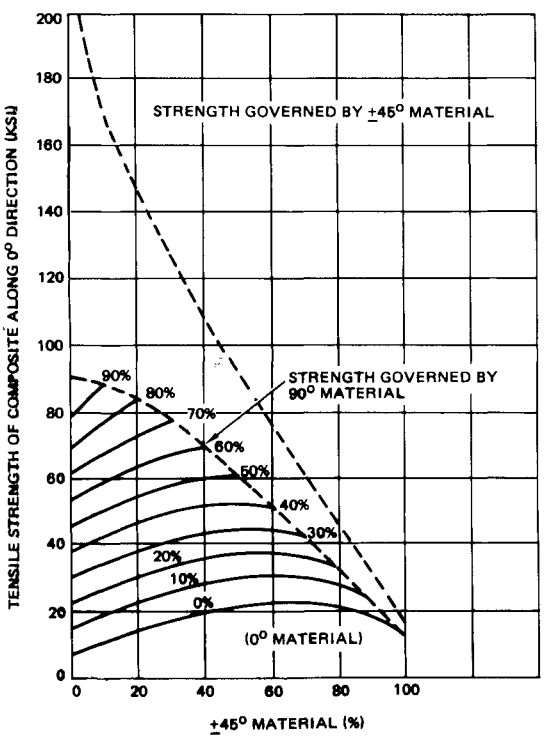

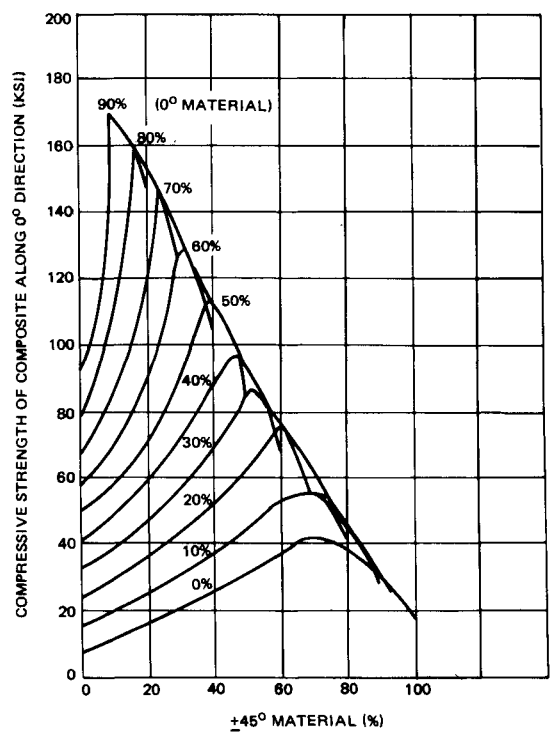

Fig. 12 Theoretically predicted mechanical properties of multilayer hybrid composites.

Table 5 Test-theory comparison of the mechanical properties of 0.5-in. thick, multilayer hybrid composites

Property		Test data[a]	Theory	Test theory
Young's modulus	$E_x \times 10^{-6}$ psi	13.04	13.1	0.996
Young's modulus	$E_y \times 10^{-6}$ psi	4.17	4.5	0.927
Shear modulus	$G_{xy} \times 10^{-6}$ psi	5.09	5.0	1.017
Poisson's ratio	ν_{xy}	0.766	0.78	0.982
Poisson's ratio	ν_{yx}	0.244	0.27	0.904
Tensile strength	$\sigma_x \times 10^{-3}$ psi	105.8	106.0	0.997
Tensile strength	$\sigma_y \times 10^{-3}$ psi	15.0[b]	21.0	0.713
Compressive strength	$\sigma_x \times 10^{-3}$ psi	94.8	98.0	0.967
Compressive strength	$\sigma_y \times 10^{-3}$ psi	21.7	25.0	0.868
Shear strength	$\sigma_{xy} \times 10^{-3}$ psi	...	21.0	...

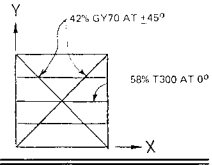

[a] Each data point is an average of at least three tests. [b] Failures were near the doubler (see Fig. 10); specimens may have contained cracks.

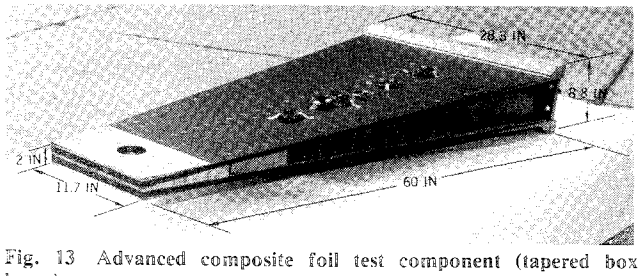

Fig. 13 Advanced composite foil test component (tapered box beam).

centrated load is to be applied during testing. The final configuration of the box beam test component is shown in Fig. 13. The hybrid composite skins are bolted and bonded to the steel substructure. Selection of this manner of attachment was based on strength and reliability considerations. At the root end, the box beam contains a metal scarf joint for attaching it to the test fixture. Extensive analytical and experimental studies were conducted to verify the loadcarrying ability of the steel-composite scarf joint. Types of experimental evaluations made on the full-size scarf joint included static tensile strength tests, static compressive strength tests, and tensile fatigue tests. The average loadcarrying ability per inch of width of the joint was found to be 36,100 lb in tension and 36,800 lb in compression. To verify the attachment between the hybrid composite skins and the metal substructure, test specimens in the form of steel I-beams reinforced with hybrid composite caps were fabricated and tested under static flexure and flexure fatigue. The composite caps were 0.5 in. thick and were attached to 3-in. high steel I-beams by bolting and bonding. These tests verified the efficiency and reliability of the attachment technique.

Extensive nondestructive evaluations were made of the box beam and its subcomponents during fabrication. The composite box beam skins (including the scarf joint) were inspected using ultrasonic through transmission and dye penetrants. Steel components and welds were inspected using x-rays. The assembled box beam was inspected for bond conditions between the skins and steel substructure using manual-contact pulse echo and a Fokker Bondtester. Appropriate standards were prepared to aid in verifying the detection capabilities of the various NDE techniques. No critical defects or anomalies were found during NDE.

The box beam is designed to fail when a 130-kip concentrated load is applied on the loading plate. The corresponding bending moment at the root end is 7.3×10^6 in.-lb, whereas the tensile and compressive loads acting on the root-end scarf joint are $\approx 1 \times 10^6$ lb. Comparison of the overall weight of the hybrid composite box beam (including joints) with an identical, equal-strength box beam made of steel shows a 34% weight saving. Realizing, however, that the massive root-end joint exists primarily to accommodate the test fixture and that the steel loading plate is only for testing purposes, it appears more meaningful to compare the weights of the hybrid composite box beam and steel box beam at their midlengths. Such a comparison shows the hybrid composite box beam to be 59% lighter than the steel box beam.

Presently, the box beam is being readied for static and fatigue testing. The experimental results on hybrid composites, box-beam structural components, and the box beam itself support the conclusions of previously reported paper studies[1,2,4] as well as the results presented in this paper regarding the efficiency and cost-effectiveness of advanced composites for application to hydrofoils and other advanced naval hydrostructures.

Acknowledgment

The work described herein was sponsored by the U.S. Naval Ship Systems Command, Washington, D.C., under contracts N00024-72-C-5536 and N00024-74-C-5441.

References

[1] Greszczuk, L. B., Hawley, A. V., and White, T., "Advanced Composites and Their Application to Hydrofoils." AIAA Paper 74-331, San Diego, California, Feb. 25-27, 1974; also published in *Journal of Hydronautics*, Vol. 9, July 1975, pp. 81-90.

[2] Greszczuk, L. B. and Hawley, A. V., "Advanced Composites and Their Application to Patrol Craft Hydrofoils," final report on work performed for U.S. Naval Ship Systems Command under Contract N00024-72-5536, April 1973.

[3] "PCH-1 MOD-1 Detail Design Structural Summary," Report D2-133900-2, prepared for Naval Ship Systems Command by The Boeing Company, June 1969.

[4] Greszczuk, L. B. and Hawley, A. V., "Application of Advanced Composites to Hydrofoil Strut," final report on work performed for U.S. Naval Ship Systems Command under Contract N00024-72-5536, Dec. 1973.

[5] "Advanced Composites Design Guide," Volume 1, Book 1, 3rd Edition, prepared by North American Rockwell Corporation under USAF Contract No. F333615-71-C-1362, Nov. 1971.

[6] Greszczuk, L. B., "Failure Criteria for Three Dimensional Orthotropic Solids," Douglas Aircraft Company, Rept. DAC 60869, Oct. 1967.

[6] Macander, A. B. and Silvergleit, M., "The Effect of Marine Environment on Stressed and Unstressed Graphite/Epoxy Composites," *Naval Engineering Journal*, Vol. 89, Aug. 1977.